In: *Methods in Neuronal Modeling* (2nd Edition),
Edited by Koch, C. and Segev, I.
MIT Press, Cambridge, MA, 1998, p. 1-25

CHAPTER 1

KINETIC MODELS OF SYNAPTIC TRANSMISSION

Alain Destexhe[1], Zachary F. Mainen[2] and Terrence J. Sejnowski[3]

1 Introduction: the kinetic interpretation of ion channel gating

The remarkably successful quantitative description of the action potential introduced by Hodgkin and Huxley (1952) is still widely used over 40 years since its introduction. The classical Hodgkin-Huxley description was not only accurate, it was also readily extensible to many other voltage-dependent currents. More recent single channel recording techniques (Sakmann and Neher, 1995) have been used to prove that voltage-dependent currents arise from populations of individual ion channels undergoing rapid transitions between conducting and non-conducting states. The macroscopic behavior of the currents can be accurately captured using kinetic models that describe the transitions between conformational states of these ion channels. This class of models, of which the Hodgkin-Huxley model is an instance, are commonly known as *Markov models.*

Kinetic models not only provide good descriptions of voltage-dependent ionic currents but are general enough to describe almost all processes essential to neurophysiology. We will focus in this chapter on synaptically-gated currents of all kinds, including neuromodulators, which are readily modeled by Markov kinetics. Moreover, many important biochemical reactions, including second-messenger systems, synaptic release, and enzymatic cascades can also be described by kinetic schemes. As a consequence, kinetic models provide means to build coherent neural models in which subcellular, cellular, and network properties are described within the same formalism (see Destexhe et al., 1994c).

Kinetic models are inherently flexible in their level of detail, ranging from the most detailed and biophysically realistic gating models to highly simplified representations. Some detailed models determined from voltage-clamp studies have more than a dozen states (e.g.,

[1]to whom correspondence should be addressed at: Laboratoire de Neurophysiologie, Faculté de Médecine, Université Laval, Québec, Canada G1K 7P4

[2]Cold Spring Harbor Laboratory, Cold Spring Harbor, NY 11724, USA

[3]The Howard Hughes Medical Institute, The Salk Institute, 10010 North Torrey Pines Road, La Jolla, CA 92037, USA, and Department of Biology, University of California San Diego, La Jolla, CA 92037, USA

Voltage-dependent gating (Hodgkin-Huxley)	$C \underset{\beta(V)}{\overset{\alpha(V)}{\rightleftharpoons}} O$
Calcium-dependent gating	$C + n\ Ca_i \underset{\beta}{\overset{\alpha}{\rightleftharpoons}} O$
Transmitter gating	$C + n\ T \underset{\beta}{\overset{\alpha}{\rightleftharpoons}} O$
Second-messenger gating	$C + n\ G \underset{\beta}{\overset{\alpha}{\rightleftharpoons}} O$

Table 1:
Most simple kinetic schemes to represent the gating of different classes of ion channels. *Voltage-dependent channels*: the channel is assumed to have opened (O) and closed (C) states modulated by voltage-dependent transition rates (α and β). *Calcium-dependent channels*: in this case, the opening of the channel depends on the binding of one or several intracellular Ca^{2+} ions (Ca_i). *Transmitter-gated channels*: molecules of neurotransmitter (T) are released transiently and bind to the channel, leading to its opening. *Second messenger-gated channels*: in this case, the opening of the channel is provided by the binding of one or several intracellular second messengers (G). Kinetic equations allow to describe all these processes, which underlie electrophysiological properties and synaptic interactions, using the same formalism (see also Appendix A).

Raman and Trussell, 1992); others have been found for the gating of receptors by neurotransmitters and intracellular second messengers such as calcium. These models accurately describe the behavior of synaptic channels as measured by single-channel or macroscopic current recordings, and are appropriate for simulating patch clamp experiments.

The essential properties of ion channel activation can be captured by simplified kinetic models with just two states. The simplest kinetic models for the gating of different classes of ion channels are illustrated in Table 1. For synaptic currents (Destexhe et al., 1994b), as for voltage-dependent currents (Destexhe et al., 1994c; Destexhe, 1997), simplified kinetic models provide an efficient way to incorporate their basic properties, such as the time course of rise and decay and their summation behavior, in simulations that do not require the level of detail described above. Typical examples of this kind are simulations of networks of neurons where the most salient features of ion channel interactions must be represented with maximal computational efficiency.

In this chapter, we focus on models of synaptic interactions. We start with an overview of relatively detailed kinetic models for synaptic release (Section 2) and for representative types of synaptic currents and receptors (Section 3). We then review simplified models for these types of synaptic interactions (Section 4). Although these simplified models have fewer states than detailed kinetic representations, they exhibit essential properties of synaptic currents, such as the summation of postsynaptic currents. Finally, the simplified models are used to simulate a small network of interacting neurons that exhibit complex behavior (Section 5). These simplified models are computationally efficient (Appendix C) and may therefore prove useful in accurately representing synaptic transmission in large network simulations.

2 Presynaptic mechanisms of transmitter release

We focus first on the mechanisms underlying the release of transmitter when an action potential arrives at the presynaptic terminal. A kinetic model of the intracellular reactions leading to ejection of transmitter by the presynaptic terminal is presented and the results are compared with more simplified models.

2.1 Model of transmitter release

The exact mechanisms whereby Ca^{2+} enters the presynaptic terminal, the specific proteins with which Ca^{2+} interacts, and the detailed mechanisms leading to exocytosis represent an active area of research (e.g., Schweizer et al., 1995). It is clear that an accurate model of these processes should include the particular clustering of calcium channels, calcium diffusion and gradients, all enzymatic reactions involved in exocytosis, and the particular properties of the diffusion of transmitter across the fusion pore and synaptic cleft. For our present purpose, we use a simple model of calcium-induced release inspired by Yamada and Zucker (1992). This model of transmitter release assumed that: (a) upon invasion by an action potential, Ca^{2+} enters the presynaptic terminal due to the presence of a high-threshold Ca^{2+} current; (b) Ca^{2+} activates a calcium-binding protein which promotes release by binding to the transmitter-containing vesicles; (c) an inexhaustible supply of "docked" vesicles are available in the presynaptic terminal, ready to release; (d) the binding of the activated calcium-binding protein to the docked vesicles leads to the release of n molecules of transmitter in the synaptic cleft. The latter process is modeled here as a first-order process with a stoichiometry coefficient of n (see details in Destexhe et al., 1994c).

The calcium-induced cascade leading to the release of transmitter was described by the following kinetic scheme:

$$4\ \mathrm{Ca}^{2+} + X \underset{k_u}{\overset{k_b}{\rightleftharpoons}} X^* \tag{1}$$

$$X^* + V_e \underset{k_2}{\overset{k_1}{\rightleftharpoons}} V_e^* \xrightarrow{k_3} n\,T\ . \qquad (2)$$

Calcium ions bind to a calcium-binding protein, X, with a cooperativity factor of 4 (see Augustine and Charlton, 1986; and references therein), leading to an activated calcium-binding protein, X^* (Eq. 1). The associated forward and backward rate constants are k_b and k_u. X^* then reversibly binds to transmitter-containing vesicles, V_e, with corresponding rate constants k_1 and k_2 (Eq. 2). The last step of this reaction, governed by rate constant k_3, represents the (irreversible) release of n molecules of transmitter, T, from the activated vesicles into the synaptic cleft. The values of the parameters in this reaction scheme were based on previous models and measurements (Yamada and Zucker, 1992).

The concentration of the liberated transmitter in the synaptic cleft, $[T]$, was approximated as follows. $[T]$ was assumed to be uniform in the cleft and cleared by processes of diffusion outside the cleft (to the extrajunctional extracellular space), uptake or degradation. These contributions were modeled by the first order reaction:

$$T \xrightarrow{k_c} \ldots \qquad (3)$$

where k_c is the rate constant for clearance of T. The values of rate constants were k_b = $10^5\ s^{-1}mM^{-4}$, k_u = $100\ s^{-1}$, k_1 = $10^6\ s^{-1}mM^{-1}$, k_2 = $100\ s^{-1}$, k_3 = $4000\ s^{-1}$, V_e = $0.01\ mM$, k_c = $10^4\ s^{-1}$ with a maximal concentration of calcium-binding proteins of $0.001\ mM$, and the number of transmitter molecules per vesicle was n = 10 000 (see Destexhe et al., 1994c).

Figure 1 shows a simulation of this model of transmitter release associated to a single compartment presynaptic terminal containing mechanisms for action potentials, high-threshold calcium currents and calcium dynamics (see Destexhe et al., 1994c for details). Injection of a short current pulse into the presynaptic terminal elicited a single action potential (Fig. 1A). The depolarization of the action potential activated high-threshold calcium channels, producing a rapid influx of calcium. The elevation of intracellular $[Ca^{2+}]$ (Fig. 1B) was transient due to clearance by an active pump. Figure 1C shows that the time-course of activated calcium-binding proteins and vesicles followed closely the time-course of the transient calcium rise in the presynaptic terminal. This resulted in a brief ($\approx 1\ ms$) rise in transmitter concentration the synaptic cleft (Fig. 1D). The rate of transmitter clearance was adjusted to match the time course of transmitter release estimated from patch clamp experiments (Clements et al., 1992; Clements, 1996) as well as for detailed simulations of extracellular diffusion of transmitter (Bartol et al., 1991; Destexhe and Sejnowski, 1995).

2.2 Further simplification of the release process

The above-described release model would be computationally very expensive if it had to be used in simulations involving thousands of synapses. Therefore, for simulating large-scale networks, simplification of the release process is needed.

The first alternative is to use a continuous function to transform the presynaptic voltage into transmitter concentration (Destexhe et al., 1994c). This approach assumes that all

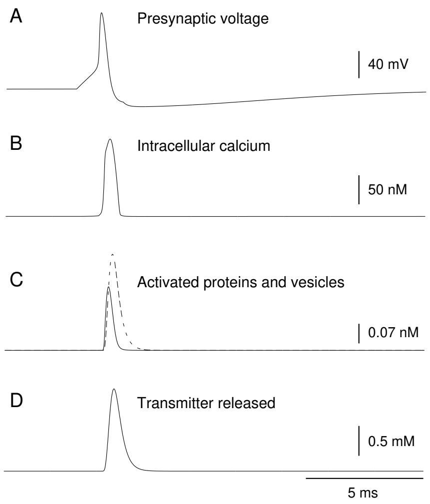

Figure 1:
Kinetic model of presynaptic release. A. A presynaptic action potential was elicited by injection of a 0.1 nA current pulse lasting 2 ms in the presynaptic terminal. B. Intracellular Ca^{2+} concentration in the presynaptic terminal. A high-threshold calcium current was also present and provided a transient calcium influx during the action potential. Removal was provided by an active calcium pump. C. Relative concentration of activated calcium-binding protein X^* (solid line) and vesicles V_e^* (dotted line). D. Concentration of transmitter in the synaptic cleft. Modified from Destexhe et al., 1994c.

intervening reactions in the release process are relatively fast and can be considered in steady state. The stationary relationship between the transmitter concentration $[T]$ and presynaptic voltage was fit to:

$$[T](V_{pre}) \quad = \quad \frac{T_{max}}{1 + \exp[-(V_{pre} - V_p)/K_p)} \tag{4}$$

where T_{max} is the maximal concentration of transmitter in the synaptic cleft, V_{pre} is the presynaptic voltage, $K_p = 5\ mV$ gives the steepness and $V_p = 2\ mV$ sets the value at which the function is half-activated. One of the main advantages of using Eq. (4) is that it provides a very simple and smooth transformation between presynaptic voltage and transmitter concentration. This form, in conjunction with simple kinetic models of postsynaptic channels, provides a model of synaptic interaction based on autonomous differential equations with only one or two variables (see also Wang and Rinzel, 1992).

The second alternative is to assume that the change in the transmitter concentration occurs in a brief pulse (Destexhe et al., 1994b). This procedure is considered in more detail in Section 4.

3 Markov models of postsynaptic currents

Conventional synaptic transmission in the central nervous system is mediated by excitatory and inhibitory amino acid neurotransmitters, glutamate and GABA, respectively. Glutamate activates AMPA/kainate receptors, responsible for most fast excitatory transmission, and NMDA receptors, whose activation is both much slower than that of AMPA/kainate receptors and whose voltage dependence may be involved in synaptic plasticity. GABA also activates two classes of receptors, $GABA_A$ receptors which have relatively fast kinetics and $GABA_B$ receptors which are much slower and involve second messengers.

It is important to note that there exists a considerable range of physiological subtypes within a given receptor class that arise from the exact molecular composition of the receptor. Most importantly, it has been shown that various properties of receptors are altered by variations in the particular subunits that make up a receptor. For example, NMDA receptor properties depend on the NR2 subunit type (A,B,C or D), which alters the Mg^{2+}sensitivity and kinetics of the channel (Monyer et al., 1994). Similarly, the presence of the GluR-B subunit determines the Ca^{2+}permeability of AMPA receptors (Jonas et al., 1994), while the GluR-B and GluR-D subunits affect their desensitization (Mosbacher et al., 1994). It has been shown that interneurons and principal cells express AMPA receptor channels with distinct subunit composition and hence distinct properties — interneurons express faster, more Ca^{2+}permeable AMPA receptors (Geiger et al., 1995). The subunit composition of receptors in different cell types and brain regions is currently the subject of intense study (see reviews by McKerran and Whiting, 1996; Huntley et al., 1994; Molinoff et al., 1994; Zukin and Bennett, 1995). Although the results of these molecular studies will undoubtedly continue to shape our understanding, for the purposes of this Chapter, we will focus on the general classes of receptors and their prototypical properties.

The study of central synapses is difficult due to inaccessibility, rapid kinetics, the difficulty of measuring or controlling the time course of neurotransmitter, and the electrotonically remote location of synapses from somatic recording sites. Nevertheless, progress in understanding the gating of these receptors has been made through the fast perfusion of transmitter to excised membrane patches containing receptors (Franke et al., 1987). With these and other methods, is has been shown that the time course of neurotransmitter in the synaptic cleft is very brief (Clements et al., 1992; Clements, 1996) and that the kinetics of the postsynaptic receptor are responsible for the prolonged time course of the slower synaptic currents (Lester et al. 1990).

Detailed models of synaptic currents based on activation by a very brief increase in transmitter concentration must capture three main aspects of receptor gating kinetics:

- *Activation/binding.* The time course of the rising phase of the synaptic current can be determined either by the rate of opening after transmitter is bound to the receptor, or, at low concentrations, the amount of transmitter present. The rising phase can be delayed (made more sigmoidal) by requiring more than one transmitter molecule to be bound (analogous to the gating of the "delayed-rectifier" potassium channel).

- *Deactivation/unbinding.* The time course of decay can be determined by either deactivation following transmitter removal or desensitization (see below). The rate of deactivation is limited either by the closing rate of the receptor, or typically, by the rate of unbinding of transmitter from the receptor.

- *Desensitization.* Synaptic receptor-gated channels can be closed by entering a so-called "desensitized" state which is analogous to the "inactivated" states of voltage-gated channels. Desensitization decreases the fraction of channels that open during a synaptic response and can affect the synaptic time course in several ways, including prolonging the decay time and shortening the rise time.

Because there are a finite number of channels at the postsynaptic membrane and they may have multiple closed and desensitized states, the dynamics that occurs during a sequence of rapid activations can be complex:

- *Priming.* Due to slow activation kinetics, a pulse of neurotransmitter may bind to but not open a channel; this can prime the receptor for response to a subsequent pulse. For GABA_B responses, this priming can occur through G-proteins on the K^+ channels (Destexhe and Sejnowski, 1995; see Section 3.4).

- *Desensitization.* A response that leads to significant desensitization may leave many receptors unable to open when neurotransmitter is released again shortly thereafter, causing a progressive decline in responsivity.

- *Saturation.* When a large fraction of receptors are bound by an initial pulse of neurotransmitter, subsequent pulses can produce greatly diminished responses since most channels are already open.

Thus, receptor kinetics are important not only in determining the time course of individual synaptic events, but also in the temporal integration during a sequence of synaptic events. In the following subsections, we review detailed kinetic schemes for the main receptor types mediating synaptic transmission in the central nervous system.

3.1 AMPA/kainate receptors

AMPA/kainate receptors mediate the prototypical fast excitatory synaptic currents in the brain. In specialized auditory nuclei AMPA/kainate receptor kinetics may be extremely rapid with rise and decay time constants in the submillisecond range (Raman et al., 1994). In the cortex and hippocampus responses are somewhat slower (e.g., Hestrin et al., 1990). The 10%-90% rise time of the fastest currents measured at the soma (representing those with least cable filtering) is 0.4 to 0.8 ms in cortical pyramidal neurons, while the decay time constant is about 5 ms (e.g., Hestrin, 1993). It may be worth noting that inhibitory interneurons express AMPA receptors with significantly different properties. First, they are about twice as fast in rise and decay time as those on pyramidal neurons (Hestrin, 1993) and second, they have a significant Ca^{2+} permeability (Koh et al., 1995). The latter property appears to be conferred by the lack of the GluRB subunit in these receptors.

The rapid time course of AMPA/kainate responses is thought to be due to a combination of rapid clearance of neurotransmitter and rapid channel closure (Hestrin, 1992). Desensitization of these receptors does occur but is somewhat slower than deactivation. The physiological significance of AMPA receptor desensitization has not been well established. Although desensitization may contribute to the fast synaptic depression observed at neocortical synapses (Thomson and Deuchars, 1994; Markram and Tsodyks, 1996), a study of paired-pulse facilitation in the hippocampus suggested a minimal contribution of desensitization even at 7 ms intervals (Stevens and Wang, 1995).

A Markov kinetic model that accounts for these properties was introduced by Patneau and Mayer (1991) (see also Jonas et al., 1993) and had the following state diagram:

$$\begin{array}{ccccccc} C_0 & \underset{R_{u_1}}{\overset{R_b\,T}{\rightleftarrows}} & C_1 & \underset{R_{u_2}}{\overset{R_b\,T}{\rightleftarrows}} & C_2 & \underset{R_c}{\overset{R_o}{\rightleftarrows}} & O \\ & & R_d \downarrow\uparrow R_r & & R_d \downarrow\uparrow R_r & & \\ & & D_1 & & D_2 & & \end{array} \qquad (5)$$

where the unbound form of the receptor C_0 binds to one molecule of transmitter T, leading to the singly-bound form C_1, which itself can bind another molecule of T leading to the doubly-bound form C_2. R_b is the binding rate and R_{u_1} and R_{u_2} are unbinding rates. Each form C_1 and C_2 can desensitize, leading to forms D_1 and D_2 with rates R_d and R_r for desensitization and resensitization respectively. Finally, the doubly-bound receptor C_2 can open, leading to the open form O, with opening and closure rates of R_o and R_c respectively. This model was simulated with the mechanism for transmitter release described in Section 2.1 and the its parameters were optimized by direct fitting of the full model to whole-cell recorded AMPA currents (see Appendix B). The fitting procedure gave the following values for the rate constants (Fig 2A): $R_b = 13 \times 10^6\ M^{-1}\ s^{-1}$, $R_{u_1} = 5.9\ s^{-1}$, $R_{u_2} = 8.6 \times 10^4\ s^{-1}$, $R_d = 900\ s^{-1}$, $R_r = 64\ s^{-1}$, $R_o = 2.7 \times 10^3\ s^{-1}$ and $R_c = 200\ s^{-1}$.

The AMPA current is then given by:

$$I_{AMPA} \;=\; \bar{g}_{AMPA}\,[O]\,(V - E_{AMPA}) \qquad (6)$$

where $\bar{g}_{AMPA}$ is the maximal conductance, $[O]$ is the fraction of receptors in the open state, V is the postsynaptic voltage and $E_{AMPA} = 0\ mV$ is the reversal potential. In neocortical and hippocampal pyramidal cells, measurements of miniature synaptic currents (10-30 pA amplitude; see McBain and Dingledine, 1992; Burgard and Hablitz, 1993) and quantal analysis (e.g., Stricker et al., 1996) lead to estimates of maximal conductance around 0.35 to 1.0 nS for AMPA-mediated currents in a single synapse.

3.2 NMDA receptors

NMDA receptors mediate synaptic currents that are substantially slower than AMPA/-kainate currents, with a rise time of about 20 ms and decay time constants of about 25 and 125 ms at 32 $°C$ (Hestrin et al., 1990). The slow kinetics of activation is due to the requirement that two agonist molecules must bind to open the receptor, as well as a relatively slow channel opening rate of bound receptors (Clements and Westbrook, 1991). The slowness of decay is believed to be due primarily to slow unbinding of glutamate from the receptor (Lester and Jahr, 1992; Bartol and Sejnowski, 1993). The open probability of an NMDA channel at the peak of a synaptic response has been estimated to be as high as 0.3 (Jahr, 1992), raising the possibility that significant saturation of synaptic NMDA receptors may occur during high-frequency stimulus trains.

An unique and important property of the NMDA receptor channel is its sensitivity to block by physiological concentrations of Mg^{2+} (Nowak et al., 1984; Jahr and Stevens, 1990a, 1990b). The Mg^{2+} block is voltage-dependent, allowing NMDA receptor channels to conduct ions only when depolarized. The necessity of both presynaptic and postsynaptic gating conditions (presynaptic neurotransmitter and postsynaptic depolarization) make the NMDA receptor a molecular coincidence detector. Furthermore, NMDA currents are carried partly by Ca^{2+} ions, which have a prominent role in triggering many intracellular biochemical cascades. Together, these properties are crucial to the NMDA receptor's role in synaptic plasticity (Bliss and Collingridge, 1993) and activity-dependent development (Constantine-Paton et al., 1990).

Several kinetic schemes have been proposed for the NMDA receptor (Clements and Westbrook, 1991; Lester and Jahr, 1992; Edmonds and Colquhoun, 1992; Clements et al., 1992; Hessler et al., 1993). These models were essentially based on the same state diagram:

$$\begin{array}{ccccccc} C_0 & \underset{R_u}{\overset{R_b\,T}{\rightleftharpoons}} & C_1 & \underset{R_u}{\overset{R_b\,T}{\rightleftharpoons}} & C_2 & \underset{R_c}{\overset{R_o}{\rightleftharpoons}} & O \\ & & & & R_d \downarrow\uparrow R_r & & \\ & & & & D & & \end{array} \tag{7}$$

This kinetic scheme is similar to that of AMPA receptors (Eq. 5), with only one desensitized form of the receptor (D) and a single unbinding rate R_u. Direct fitting of this model to whole-cell recorded NMDA currents (in free Mg^{2+}; see below) gave the following values for the rate constants (Fig 2B): $R_b = 5 \times 10^6\ M^{-1}\ s^{-1}$, $R_u = 12.9\ s^{-1}$, $R_d = 8.4\ s^{-1}$, $R_r = 6.8\ s^{-1}$, $R_o = 46.5\ s^{-1}$ and $R_c = 73.8\ s^{-1}$.

The NMDA current is then described by:

$$I_{NMDA} \;=\; \bar{g}_{NMDA}\ B(V)\ [O]\ (V - E_{NMDA}) \tag{8}$$

where $\bar{g}_{NMDA}$ is the maximal conductance, $B(V)$ is the magnesium block (see below), $[O]$ is the fraction of receptors in the open state, V is the postsynaptic voltage and $E_{NMDA} = 0\ mV$ is the reversal potential.

Miniature excitatory synaptic currents also have an NMDA-mediated component (McBain and Dingledine, 1992; Burgard and Hablitz, 1993) and the conductance of dendritic NMDA channels have been reported to be a fraction of AMPA channels, between 3 to 62% (Zhang and Trussell, 1994; Spruston et al., 1995), leading to estimates of the maximal conductance of NMDA-mediated currents at a single synapse around $\bar{g}_{NMDA} = 0.01 - 0.6\ nS$.

The magnesium block of the NMDA receptor channel is an extremely fast process compared to the other kinetics of the receptor (Jahr and Stevens, 1990a, 1990b). The block can therefore be accurately modeled as an instantaneous function of voltage (Jahr and Stevens, 1990b):

$$B(V) \;=\; \frac{1}{1 + \exp(-0.062\ V)\ [\mathrm{Mg}^{2+}]_o / 3.57} \tag{9}$$

where $[\mathrm{Mg}^{2+}]_o$ is the external magnesium concentration (1 to 2 mM in physiological conditions).

3.3 GABA$_A$ receptors

Most fast inhibitory postsynaptic potentials (IPSPs) are mediated by GABA$_A$ receptors in the central nervous system. GABA$_A$-mediated IPSPs are elicited following minimal stimulation, in contrast to GABA$_B$ responses which require strong stimuli (see Section 3.4). GABA$_A$ receptors have a high affinity for GABA and are believed to be saturated by release of a single vesicle of neurotransmitter (see Mody et al., 1994; Thompson, 1994). GABA$_A$ receptors have at least two binding sites for GABA and show a weak desensitization (Busch and Sakmann, 1990; Celentano, 1994). However, blocking uptake of GABA reveals prolonged GABA$_A$ currents that last for more than a second (Thompson and Gähwiler, 1992; Isaacson et al., 1993), suggesting that, as with AMPA/kainate receptors, deactivation following transmitter removal is the main determinant of the decay time.

We used the kinetic model introduced by Busch and Sakmann (1990) for GABA$_A$ receptors based on the following state diagram:

$$\begin{array}{ccccc} C_0 & \underset{R_{u_1}}{\overset{R_{b_1}\,T}{\rightleftharpoons}} & C_1 & \underset{R_{u_2}}{\overset{R_{b_2}\,T}{\rightleftharpoons}} & C_2 \\ & & R_{o_1} \Big\downarrow\!\Big\uparrow R_{c_1} & & R_{o_2} \Big\downarrow\!\Big\uparrow R_{c_2} \\ & & O_1 & & O_2 \end{array} \tag{10}$$

Here, the transmitter GABA (T) binds to the unbound form C_0, leading to singly-bound C_1 and doubly-bound form C_2, with binding and unbinding rates R_{b_1}, R_{u_1}, R_{b_2} and R_{u_2} respectively. Both singly- and doubly-bound forms can open, leading to O_1 and O_2 forms with opening and closure rates of R_{o_1}, R_{c_1}, R_{o_2} and R_{c_2} respectively. Direct fitting of this model to whole-cell recorded GABA$_A$ currents gave the following values for the rate constants (Fig 2C): $R_{b_1} = 20 \times 10^6\ M^{-1}\ s^{-1}$, $R_{u_1} = 4.6 \times 10^3\ s^{-1}$, $R_{b_2} = 10 \times 10^6\ M^{-1}\ s^{-1}$, $R_{u_2} = 9.2 \times 10^3\ s^{-1}$, $R_{o_1} = 3.3 \times 10^3\ s^{-1}$, $R_{c_1} = 9.8 \times 10^3\ s^{-1}$, $R_{o_2} = 10.6 \times 10^3\ s^{-1}$ and $R_{c_2} = 410\ s^{-1}$.

The current is then given by:

$$I_{GABA_A} \;=\; \bar{g}_{GABA_A}\,([O_1] + [O_2])\,(V - E_{Cl}) \tag{11}$$

where $\bar{g}_{GABA_A}$ is the maximal conductance, $[O_1]$ and $[O_2]$ are the fractions of receptors in the open states, and $E_{Cl} = -70\ mV$ is the chloride reversal potential. Estimation of the maximal conductance at a single GABAergic synapse from miniature GABA$_A$-mediated currents (Ropert et al., 1990; De Koninck and Mody, 1994) leads to $\bar{g}_{GABA_A} = 0.25{-}1.2\,nS$.

3.4 GABA$_B$ receptors

In the three types of synaptic receptors discussed so far, the receptor and ion channel are both part of the same protein complex. In contrast, other classes of synaptic response

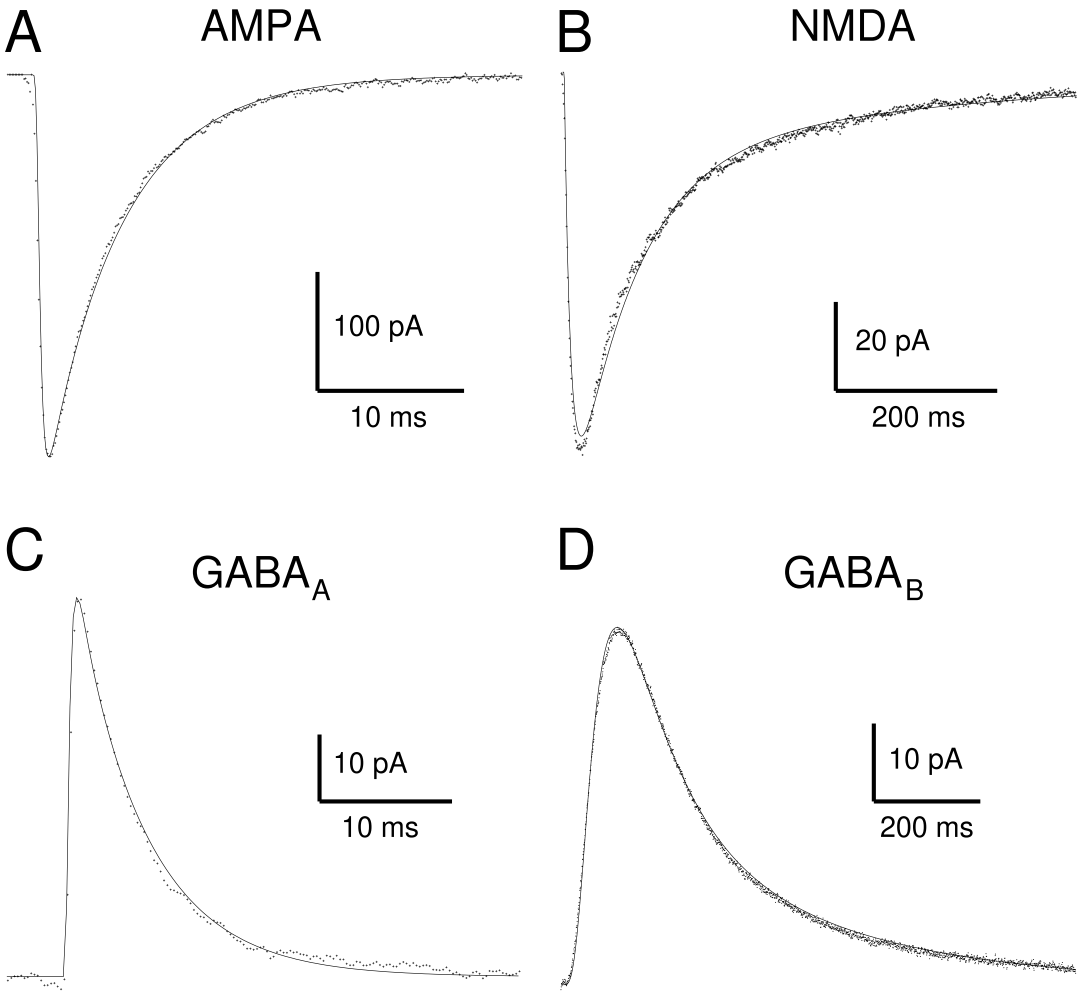

Figure 2:
Best fits of detailed kinetic models to averaged postsynaptic currents obtained from whole-cell recordings. A. AMPA/kainate-mediated currents (obtained from Xiang et al., 1992; recorded at 31 $°C$). B. NMDA-mediated currents (obtained from Hessler and Malinow, 1993; recorded at 22-25 $°C$ in Mg^{2+}-free solution). C. $GABA_A$-mediated currents. D. $GABA_B$-mediated currents (C-D recorded at 33-35 $°C$ by Otis et al., 1992; 1993). For all graphs, the averaged recording of the synaptic current (noisy trace) is represented with the best fit obtained using the models (continuous trace). Models are described in the text; transmitter release was modeled as in Fig. 1. D modified from Destexhe and Sejnowski, 1995; fitting procedures described in Appendix B).

are mediated by an ion channel that is not directly coupled to a receptor, but rather is activated (or deactivated) by an intracellular "second messenger" that is produced when neurotransmitter binds to a separate receptor molecule. This is the case for GABA$_B$ receptors, whose response is mediated by K^+ channels that are activated by G-proteins (Dutar and Nicoll, 1988).

Unlike GABA$_A$ receptors which respond to weak stimuli, responses from GABA$_B$ responses require high levels of presynaptic activity (Dutar and Nicoll, 1988; Davies et al., 1990; Huguenard and Prince, 1994). This property might be due to extrasynaptic localization of GABA$_B$ receptors (Mody et al., 1994), but a detailed model of synaptic transmission on GABAergic receptors suggests that this effect could also be due to cooperativity in the activation kinetics of GABA$_B$ responses (Destexhe and Sejnowski, 1995; see "Priming" in Section 3). Typical properties of GABA$_B$-mediated responses in hippocampal and thalamic slices can be reproduced assuming that several G-proteins bind to the associated K^+ channels (Destexhe and Sejnowski, 1995), leading to the following scheme:

$$
\begin{aligned}
R_0 + T &\rightleftharpoons R \rightleftharpoons D && (12)\\
R + G_0 &\rightleftharpoons RG \longrightarrow R + G && (13)\\
G &\longrightarrow G_0 && (14)\\
C_1 + n\,G &\rightleftharpoons O && (15)
\end{aligned}
$$

Here the transmitter, T, binds to the receptor, R_0, leading to its activated form, R, and desensitized form, D. The G-protein is transformed from an inactive (GDP-bound) form, G_0, to an activated form, G, catalyzed by R. Finally, G binds to open the K^+ channel, with n independent binding sites. If we assume quasi-stationarity in (13) and (15), and consider G_0 in excess, then the reduced kinetic equations for this system are:

$$
\begin{aligned}
\frac{d[R]}{dt} &= K_1\,[T]\,(1-[R]-[D]) - K_2\,[R] + K_3\,[D]\\
\frac{d[D]}{dt} &= K_4\,[R] - K_3\,[D]\\
\frac{d[G]}{dt} &= K_5\,[R] - K_6\,[G]\\
I_{GABA_B} &= \bar{g}_{GABA_B}\,\frac{[G]^n}{[G]^n + K_d}\,(V - E_K)
\end{aligned}
\qquad (16)
$$

where $[R]$ and $[D]$ are respectively the fraction of activated and desensitized receptor, $[G]$ (in μM) is the concentration of activated G-protein, $\bar{g}_{GABA_B} = 1\ nS$ is the maximal conductance of K^+ channels, $E_K = -95\ mV$ is the potassium reversal potential, and K_d is the dissociation constant of the binding of G on the K^+ channels. This model accounted accurately for both the time course and the properties of GABA$_B$ responses. Direct fitting of the model to whole-cell recorded GABA$_B$ currents gave the following values (Fig 2D; Destexhe and Sejnowski, 1995): $K_d = 100\ \mu M^4$, $K_1 = 6.6 \times 10^5\ M^{-1}\ s^{-1}$, $K_2 = 20\ s^{-1}$, $K_3 = 5.3\ s^{-1}$, $K_4 = 17\ s^{-1}$, $K_5 = 8.3 \times 10^{-5} M\ s^{-1}$ and $K_6 = 7.9\ s^{-1}$ with $n = 4$ binding sites.

As discussed above, $GABA_B$-mediated responses typically require high stimulus intensities to be evoked. Miniature GABAergic synaptic currents indeed never contain a $GABA_B$-mediated component (Otis and Mody, 1992; Thompson and Gähwiler, 1992; Thompson, 1994). As a consequence, $GABA_B$-mediated unitary IPSPs are difficult to obtain experimentally and the estimation of the maximal conductance of $GABA_B$ receptors in a single synapse is difficult. A peak $GABA_B$ conductance of around 0.06 nS was reported using release evoked by local application of sucrose (Otis et al., 1992).

3.5 Other neuromodulators

Neurotransmitters including glutamate (through metabotropic receptors), acetylcholine (through muscarinic receptors), noradrenaline, serotonin, dopamine, histamine, opioids, and others have been shown to mediate slow intracellular responses. These neurotransmitters induce the intracellular activation of G proteins, which may affect ionic currents as well as the metabolism of the cell. As with GABA acting on $GABA_B$ receptors, the main electrophysiological target of many neuromodulators is to open or close K^+ channels (see Brown, 1990; Brown and Birnbaumer, 1990; McCormick, 1992). The model of $GABA_B$ responses could thus be used to model these currents, with rate constants adjusted to fit the time courses reported for the particular responses. However, the data available presently are not precise enough to allow the development of detailed models of these responses. If they are similar in their kinetics to $GABA_B$, then the same model may apply as in Eqs. 16.

4 Simplified models of postsynaptic currents

It is possible to simplify the receptor kinetic models in the previous section to make them computationally more efficient while retaining the most important qualitative properties. It is also possible to greatly simplify the release process that determines the transmitter concentration T.

Voltage-clamp recordings in excised membrane patches showed that 1 ms pulses of 1 mM glutamate reproduced PSCs that were quite similar as those recorded in the intact synapse (Hestrin, 1992; Colquhoun et al., 1992; Standley et al., 1993). Assume that the transmitter, either glutamate or GABA, is released according to a pulse when an action potential invades the presynaptic terminal. Then, a two-state (open/closed) kinetic scheme, combined with such a pulse of transmitter, can be solved analytically (Destexhe et al., 1994b). The same approach also yields simplified algorithms for three-state and higher schemes (Destexhe et al., 1994c). As a consequence, extremely fast algorithms can be used to simulate most types of synaptic receptors (see also Appendix C).

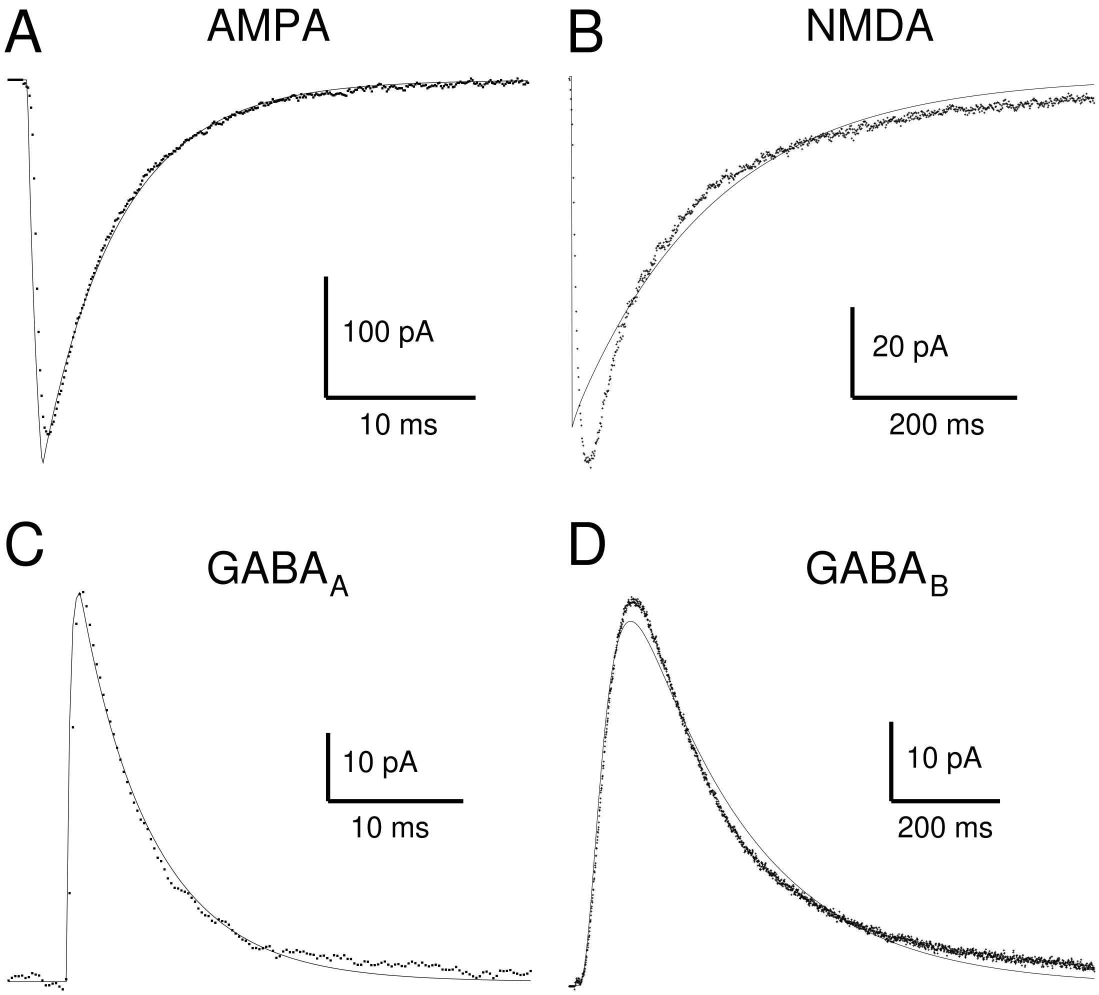

Figure 3:

Best fits of simplified kinetic models to averaged postsynaptic currents obtained from whole-cell recordings. A. AMPA/kainate-mediated currents. B. NMDA-mediated currents. C. $GABA_A$-mediated currents. D. $GABA_B$-mediated currents. For all graphs, averaged whole-cell recordings of synaptic currents (noisy traces; identical description as in Fig. 2) are represented with the best fit obtained using the simplest kinetic models (continuous traces). Transmitter time course was a pulse of 1 mM and 1 ms duration in all cases (A: modified from Destexhe et al., 1994c; C: modified from Destexhe et al., 1994a; D: modified from Destexhe et al., 1996; fitting procedures described in Appendix B).

4.1 AMPA/kainate receptors

The simplest model that approximates the kinetics of the fast AMPA/kainate type of glutamate receptors can be represented by the two-state diagram:

$$C + T \underset{\beta}{\overset{\alpha}{\rightleftharpoons}} O \tag{17}$$

where α and β are voltage-independent forward and backward rate constants. If r is defined as the fraction of the receptors in the open state, it is then described by the following first-order kinetic equation:

$$\frac{dr}{dt} = \alpha\,[T]\,(1-r) - \beta r \tag{18}$$

and the postsynaptic current I_{AMPA} is given by:

$$I_{AMPA} = \bar{g}_{AMPA}\; r\;(V - E_{AMPA}) \tag{19}$$

where $\bar{g}_{AMPA}$ is the maximal conductance, E_{AMPA} is the reversal potential and V is the postsynaptic membrane potential.

The best fit of this kinetic scheme to whole-cell recorded AMPA/kainate currents (Fig 3A) gave $\alpha = 1.1 \times 10^6\ M^{-1}s^{-1}$ and $\beta = 190\ s^{-1}$ with $E_{AMPA} = 0\ mV$.

4.2 NMDA receptors

The slower NMDA type of glutamate receptors can be represented with a two-state model similar to AMPA/kainate receptors, with a voltage-dependent term representing magnesium block (see Section 3). Using scheme in Eqs. 17 and 18, the postsynaptic current is given by:

$$I_{NMDA} = \bar{g}_{NMDA}\; B(V)\; r\;(V - E_{NMDA}) \tag{20}$$

where $\bar{g}_{NMDA}$ is the maximal conductance, E_{NMDA} is the reversal potential and $B(V)$ represents the magnesium block (same equation as Eq. 9).

The best fit of this kinetic scheme to whole-cell recorded NMDA currents (Fig 3B) gave $\alpha = 7.2 \times 10^4\ M^{-1}s^{-1}$ and $\beta = 6.6\ s^{-1}$ with $E_{NMDA} = 0\ mV$.

4.3 GABA$_A$ receptors

GABA$_A$ receptors can also be represented by the scheme in Eqs. 17 and 18, with the postsynaptic current given by:

$$I_{GABA_A} = \bar{g}_{GABA_A}\; r\;(V - E_{GABA_A}) \tag{21}$$

where $\bar{g}_{GABA_A}$ is the maximal conductance and E_{GABA_A} is the reversal potential.

The best fit of this kinetic scheme to whole-cell recorded GABA$_A$ currents (Fig 3C) gave $\alpha = 5 \times 10^6\ M^{-1}s^{-1}$ and $\beta = 180\ s^{-1}$ with $E_{GABA_A} = -80\ mV$.

4.4 GABA$_B$ receptors and neuromodulators

The stimulus dependency of GABA$_B$ responses, unfortunately, cannot be handled correctly by a two-state model. The simplest model of GABA$_B$-mediated currents has two variables and was obtained from Eqs. 16:

$$
\begin{aligned}
\frac{dr}{dt} &= K_1\,[T]\,(1-r) - K_2\,r \\
\frac{ds}{dt} &= K_3\,r - K_4\,s \\
I_{GABA_B} &= \bar{g}_{GABA_B}\,\frac{s^n}{s^n + K_d}\,(V - E_K)
\end{aligned}
\tag{22}
$$

where all symbols have the same meaning as in Eqs. 16 with $r = [R]$ and $s = [G]$. Fitting of this model to whole-cell recorded GABA$_B$ currents (Fig 3D) gave the following values: $K_d = 100\ \mu M^4$, $K_1 = 9 \times 10^4\ M^{-1}\ s^{-1}$, $K_2 = 1.2\ s^{-1}$, $K_3 = 180\ s^{-1}$ and $K_4 = 34\ s^{-1}$ with $n = 4$ binding sites.

The main difference between this model and Eqs. 16 is the absence of a desensitized state for the receptor. We found that the desensitized state was necessary to account accurately for the time course of GABA$_B$ currents (Fig 2D), but had little influence on the dynamical properties of GABA$_B$ responses (see Destexhe et al., 1996).

5 Implementation

In this section, we consider the implementation of simplified release processes together with the kinetic models of postsynaptic receptors described in Section 4. Connecting presynaptic and postsynaptic compartments can be accomplished either by using functions which approximate the release process, such as Eq. (4), or by using pulses of transmitter. In the first case, the network will be described by autonomous differential equations, which has potentially many applications for mathematical analyses. However, the drawback of this approach is that each synaptic contact gives rise to additional differential equations.

Using pulses of transmitter provides a good alternative if computational efficiency is an important concern. Typically, a pulse of transmitter is triggered at each time the presynaptic voltage crosses a given threshold (0 mV in the present examples). Taking advantage of the pulse, the equations can be solved analytically (Appendix C.1; Destexhe et al., 1994b). Therefore, no additional differential equation must be solved for postsynaptic currents. In Appendix C.2, we present an algorithm that allows simulations of models with many synapses on the same compartment to be greatly expedited (Lytton, 1996).

5.1 Synaptic summation

The summation of postsynaptic potentials (PSPs) and postsynaptic currents (PSCs) is an important aspect of synaptic signaling. Although alpha functions are often used to represent PSCs in models, these template functions were originally introduced to fit a single PSP (Rall, 1967) and consequently are inappropriate for modeling summated post-synaptic events, where they prove computationally inefficient because several waveforms

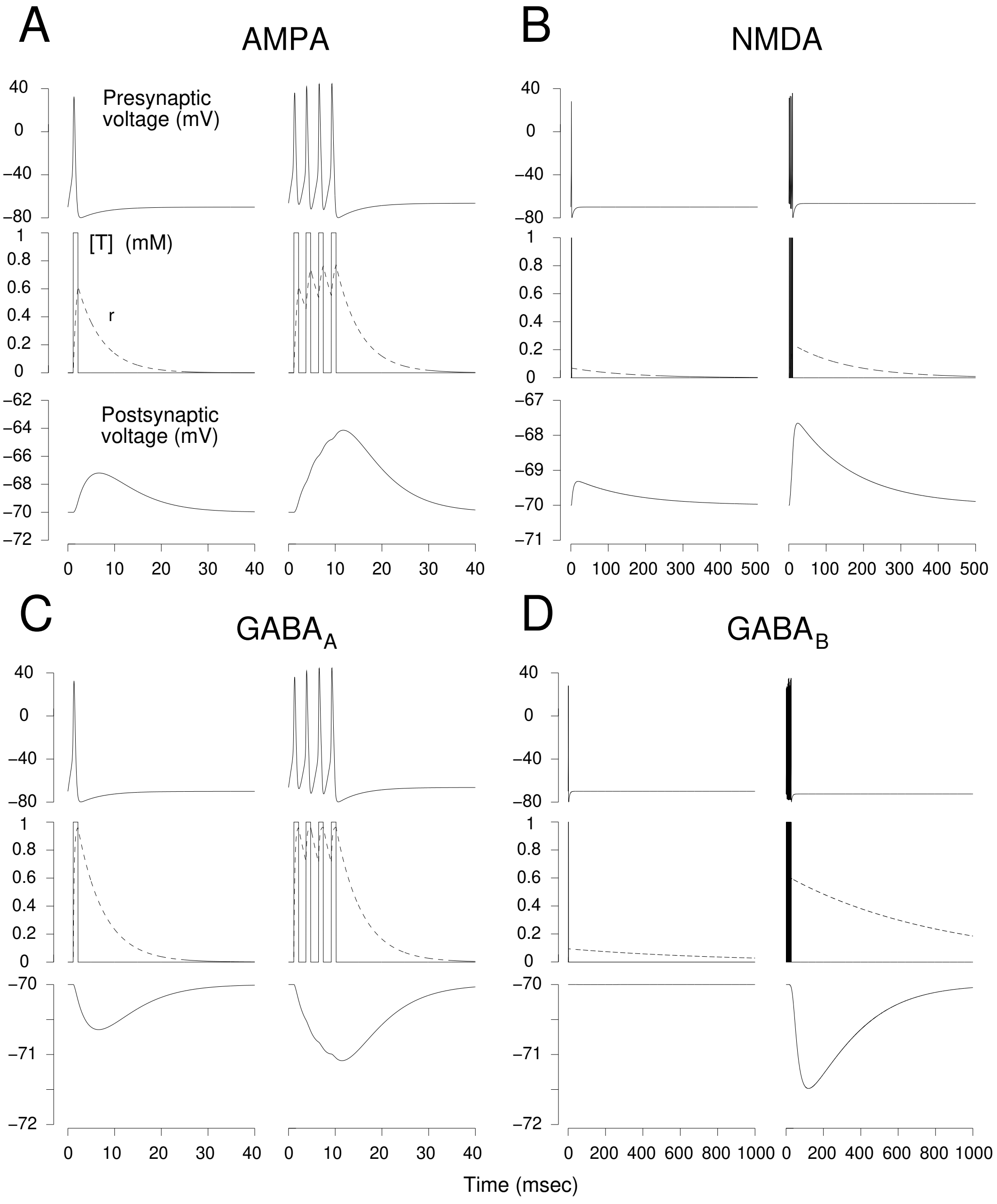

Figure 4:

Summation of postsynaptic potentials in simplified kinetic models of different receptors. A single compartment model (10 μm diameter, 10 μm length, 0.2 mS/cm^2 leak conductance and -70 mV leak reversal) was provided with postsynaptic receptors: A, AMPA/kainate receptors; B, NMDA receptors; C, GABA$_A$ receptors and D, GABA$_B$ receptors. In all cases, the behavior with one presynaptic spike (left panels) is compared with that of a burst of presynaptic spikes at high frequency (300-400 Hz; 4 spikes in A,B,C; 10 spikes in D). All synaptic conductances were of 0.1 nS; other parameters as in Section 4.

substantially overlap. Kinetic models on the other hand provide a natural way to handle summation because receptors properly integrate successive releases of neurotransmitter.

The summation behavior of simple kinetic models is shown in Fig. 4 for the simple models of the four receptor types described in Section 4. The three transmitter-gated receptor types (AMPA, NMDA and $GABA_A$) showed PSP amplitudes proportional to the number of presynaptic spikes. In this case, the membrane potential always stayed far from the reversal potential, resulting in a relatively linear summation. However, for $GABA_B$ receptors, the situation is radically different: a single presynaptic spike cannot activate enough G-protein to evoke detectable currents. On the other hand, $GABA_B$-mediated currents are reliably evoked when a burst of 10 presynaptic spikes occurs. This nonlinear stimulus dependency is typical of $GABA_B$ receptors (see Destexhe and Sejnowski, 1995 for more details).

5.2 Connecting networks

The main application of the simplified kinetic models described in Section 4 is to build network simulations. Simple kinetic models may not be able to adequately simulate the finest details of synaptic currents, but they can provide a good approximation to some of their features such as rise, decay, voltage dependence, and summation properties, while maintaining computational efficiency.

We present here an example of a simulation of thalamic oscillations that used the models described in Section 4 together with presynaptically-triggered pulses of transmitter (Destexhe et al., 1996). The occurrence of spindle oscillations depends critically on both intrinsic properties of cells and the types of synaptic receptors present in the circuitry (see Steriade et al., 1993). The minimal model for these oscillations is shown in Fig. 5. Two types of cells were present, thalamocortical (TC) relay cells and thalamic reticular (RE) cells. Both thalamic neurons displayed bursts of action potentials due to the presence of a low-threshold calcium current. Connecting these neurons with AMPA, $GABA_A$ and $GABA_B$ receptors can give rise to oscillations in the network. These behaviors could be simulated using simplified kinetic models for synaptic currents, together with models of the Hodgkin-Huxley type for voltage-dependent currents. The various properties of these oscillations, including the frequency and phase relationships between cells, were within the range of experimental measurements only when realistic values were used for the rise and decay times of synaptic currents (Destexhe et al., 1996).

It must be noted that more complex synaptic interactions can be captured by simplified models involving more than two states. For example, fast synaptic depression of excitatory connections between pyramidal cells (Markram and Tsodyks, 1996) can be captured phenomenologically using a three-state kinetic scheme that includes a desensitized state (Destexhe et al., 1994c). Such a scheme is also analytically solvable, therefore could also be used as the basis for network simulations that include fast synaptic depression.

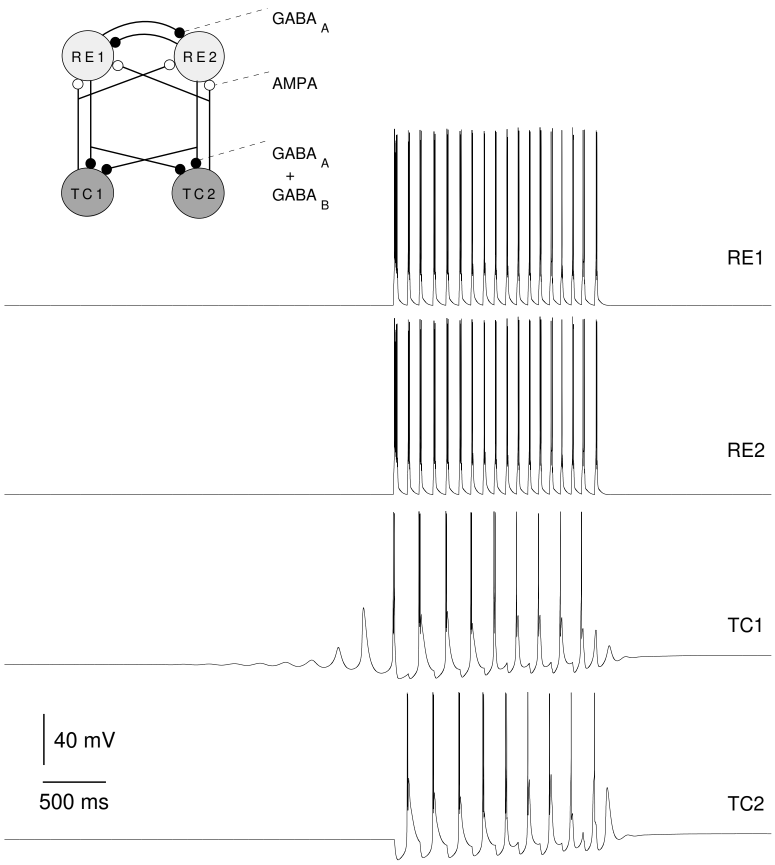

Figure 5:

Simple circuit of thalamic neurons interconnected through glutamatergic and GABAergic synapses. Both types of neurons produced bursts of action potentials due to the presence of a low threshold Ca^{2+} current and had also Na^+/K^+ currents responsible for action potential generation; a hyperpolarization-activated current (I_h) was present in TC cells. RE cells inhibited each-other through $GABA_A$ receptors and provided a mixture of $GABA_A$- and $GABA_B$-mediated IPSPs in TC cells. TC cells excited RE cells through AMPA receptors. This example was taken from a modeling study of thalamic oscillations (Destexhe et al., 1996) and was based on voltage-clamp and current-clamp data obtained in thalamic slices (Bal and McCormick, 1995a, 1995b). Oscillations occurred spontaneously in this system and were critically dependent on the kinetics of both intrinsic and synaptic currents. Hodgkin-Huxley type of models were used for voltage-dependent currents, and pulse-based kinetic models for synaptic receptors (see Section 4). All simulations were simulated with NEURON; figure modified from Destexhe et al., 1996.

Appendix

A Kinetic models of gating mechanisms

This appendix formally describes state diagrams for different types of gating, presents the corresponding kinetic equations, and explains how to relate them.

Generally, kinetic models are written as state diagrams

$$S_1 \rightleftharpoons S_2 \rightleftharpoons \dots \rightleftharpoons S_n \ , \tag{23}$$

where S_1 ... S_n represent the various states of the channel. The transition between any pair of states can be written as

$$S_i \underset{r_{ji}}{\overset{r_{ij}}{\rightleftharpoons}} S_j \ , \tag{24}$$

where r_{ij} and r_{ji} are the rate constants that govern the transition between states S_i and S_j. The fraction of channels in state S_i, s_i, obeys the relation

$$\frac{ds_i}{dt} = \sum_{j=1}^{n} s_j \ r_{ji} - \sum_{j=1}^{n} s_i \ r_{ij} \tag{25}$$

which is the conventional kinetic equation for the various states of the system.

In the case of voltage-dependent channels, the rate constants will depend on voltage:

$$S_i \underset{r_{ji}(V)}{\overset{r_{ij}(V)}{\rightleftharpoons}} S_j \ . \tag{26}$$

The voltage dependence of the rate constants can always be expressed as

$$r_{ij}(V) = \exp[-U_{ij}(V)/RT] \ , \tag{27}$$

where $U_{ij}(V)$ is the free energy barrier for the transition from state S_i to S_j, R is the gas constant and T is the absolute temperature. The exact form of $U_{ij}(V)$ is in general very difficult to ascertain, and may involve both linear and nonlinear components arising from interactions between the channel protein and the membrane electrical field (Stevens, 1978). Assuming a linear dependence of U_{ij} on voltage leads to monoexponential expressions for the rate constants, which is usually largely sufficient for modeling the voltage dependence of most types of ion channels.

In the case of ligand-gated channels, the transition between unbound and bound states of the channel depends on the concentration of ligand:

$$L + S_i \underset{r_{ji}}{\overset{r_{ij}}{\rightleftharpoons}} S_j \ . \tag{28}$$

Here, L is the ligand, S_i is the unbound state, S_j is the bound state (sometimes written S_iL), r_{ij} and r_{ji} are rate constants as defined before. The same reaction can be rewritten as:

$$S_i \underset{r_{ji}}{\overset{r_{ij}([L])}{\rightleftharpoons}} S_j \ , \tag{29}$$

where $r_{ij}([L]) = [L]\ r_{ij}$ and $[L]$ is the concentration of ligand. Written in this form, (29) is equivalent to (26). Ligand-gating schemes are generally equivalent to voltage-gating schemes, although the functional dependence of the rate constants on $[L]$ is simple compared to the voltage-dependence discussed above. For gating processes depending on intracellular calcium, or second messengers such as G proteins, the functional form is identical to (29).

All state diagrams described in Sections 3 and 4 are analogues to Eqs. 28-29 and the kinetic equations of the models are obtained using Eq. 25. Either of these forms can be used to simulate the behavior of these receptors using NEURON (Hines, 1993), which can handle state diagrams as well as differential equations.

It should be noted that the kinetic formalism is limited to the description of macroscopic phenomena, involving a large population of receptors and channels. In the case of smaller systems, in which a limited number of receptors or molecules are involved, a different formalism may be needed. For example, molecular interactions at a single release site may require to simulate the trajectories and binding of individual molecules in a three-dimensional model (Stiles et al., 1996). A general Monte Carlo simulation environment, called MCELL (Bartol et al, 1996), has been developed for exploring such models. MCELL focuses on the biochemistry of ligand/effector interactions on the time scale of microseconds to hundreds of milliseconds and the spatial scale of nanometers to tens of micrometers. It is complementary to other neurosimulation tools such as NEURON.

B Fitting kinetic models to experimental data

This appendix briefly describes the methods used to fit the kinetic models to experimental data, as in Figs. 2-3.

For simplified kinetic models with two or three states, the time course of the current can be obtained analytically assuming that the transmitter time course follows a pulse (Destexhe et al., 1994b, 1994c; see Appendix C.1). It is then straightforward to fit this expression to experimental data using a simplex least squares fitting algorithm (see Press et al., 1986). The fitting then leads to very stable and unique values of the parameters from different initial conditions.

In the case of more complex models, the current was obtained by simulating the model and fit to experimental waveforms using the simplex algorithm. At each iteration of the simplex procedure, the model was run and the least square error calculated between model and experimental traces. The optimization procedures controlled and adjusted the model parameters at each iteration, until minimal error was reached. This procedure can be run using built-in features of the NEURON simulator (Hines, 1993).

Several sets of initial parameter values must be used in order to check for uniqueness of the optimal values obtained after the fitting procedure. In some cases, the complexity of the models and the large number of parameters can make it impossible to obtain a unique set of values. This indicates that there are not enough constraints in the experimental data to estimate the value of all parameters. In such cases, uniqueness can be achieved when not all parameters are allowed to vary, for example when known parameters, such as the forward binding constant, are fixed. In these conditions, the optimal values for parameters must always be robust to changes in initial values, within a minimal error.

C Optimized algorithms

In this appendix, we give practical algorithms for calculating synaptic currents with high computational efficiency. These algorithms are applicable to two-state models of postsynaptic currents, such as that mediated by AMPA/kainate, NMDA and $GABA_A$ receptors (cfr. Section 4).

C.1 Single synapse

The use of a pulse of transmitter allows Eq. 18 to be analytically solved during each phase of the pulse during which $[T]$ is constant (Destexhe et al., 1994b). In Eq. 18, define the following two variables:

$$r_\infty = \frac{\alpha\ T_{max}}{\alpha\ T_{max} + \beta} \quad \text{and} \quad \tau_r = \frac{1}{\alpha\ T_{max} + \beta}$$

where T_{max} is the maximal concentration of the transmitter during the pulse ($T_{max} = 1\ mM$ here).

The analytical expression for the fraction of open receptors r for each phase of the pulse can be calculated as follows:

1. When the pulse is on ($t_0 < t < t_1$), $[T] = T_{max}$ and r is given by:

$$r(t - t_0) = r_\infty + (r(t_0) - r_\infty)\ \exp[-(t - t_0)/\tau_r] \tag{30}$$

2. When the pulse is off ($t > t_1$), $[T] = 0$, and r is given by:

$$r(t - t_1) = r(t_1)\ \exp[-\beta\ (t - t_1)] \tag{31}$$

In a backward-Euler type of integration scheme, the update rule for each time step Δt is:

$$\begin{array}{rcll} r & = & r_\infty + (r - r_\infty)\ \exp[-\Delta t/\tau_r] & \text{if } [T] > 0 \\ r & = & r\ \exp[-\beta\ \Delta t] & \text{if } [T] = 0 \end{array} \tag{32}$$

The computational advantage of two-state kinetic models of synaptic currents is therefore that (a) no differential equation needs to be solved; (b) at each time step Δt, only one exponential term is evaluated, independently of the number of spikes received by the synapse. This exponential term can be precalculated, leading to further increase in computational efficiency.

C.2 Multiple synapses

Suppose that the same postsynaptic compartment receives N identical synaptic contacts from N different sources. The synaptic current at each individual contact is:

$$I_i \;=\; \bar{g}_{syn}\; r_i\; (V - E_{syn}) \tag{33}$$

where r_i is the fraction of open receptors at synapse i.

Following Eq. 32, the update rule for computing N synaptic currents at each time step Δt can be written as:

$$\begin{aligned} r_i &= r_\infty + (r_i - r_\infty)\; \exp[-\Delta t/\tau_r] && \text{if } [T]_i > 0 \\ r_i &= r_i\; \exp[-\beta\; \Delta t] && \text{if } [T]_i = 0 \end{aligned} \tag{34}$$

This update rule can be much optimized if all state variables r_i are merged together into two groups for active ($[T]_i > 0$) and inactive ($[T]_i = 0$) synapses, such that:

$$\begin{aligned} R_{on} &= \textstyle\sum_i\; r_i \quad (\text{such that all } \; [T]_i > 0) \\ R_{off} &= \textstyle\sum_i\; r_i \quad (\text{such that all } \; [T]_i = 0) \end{aligned} \tag{35}$$

and updated as:

$$\begin{aligned} R_{on} &= N_{on}\; r_\infty + (R_{on} - N_{on}\; r_\infty)\; \exp[-\Delta t/\tau_r] \\ R_{off} &= R_{off}\; \exp[-\beta\; \Delta t] \end{aligned} \tag{36}$$

where N_{on} is the number of active synapses.

At each time a pulse of transmitter begins or ends, the variables R_{on} and R_{off} must be changed accordingly. This is easily done since the value of any r_i at any time can be calculated from its value at the time it last changed. If a spike occurs at a synapse i, the following computations are performed:

$$\begin{aligned} r_i(t) &= r_i(t_0)\; \exp[-\beta\; (t - t_0)] \\ R_{on} &= R_{on} + r_i(t) \\ R_{off} &= R_{off} - r_i(t) \end{aligned} \tag{37}$$

where t_0 is the time of the preceding event that occurred at synapse i.

When the pulse of transmitter ends, the following computations are performed:

$$\begin{aligned} r_i(t) &= r_\infty + (r_i(t_0) - r_\infty)\; \exp[-(t - t_0)/\tau_r] \\ R_{on} &= R_{on} - r_i(t) \\ R_{off} &= R_{off} + r_i(t) \end{aligned} \tag{38}$$

Here t_0 is the time at which the pulse of transmitter started.

This multisynapse algorithm was introduced by Lytton (1996) and allows considerable reduction of execution time for large numbers of synapses. Benchmarks (Lytton, 1996) show that this algorithm is much faster than all other existing methods. Calculation of alpha functions, even when optimized (Srinivasan and Chiel, 1993), would require at least one exponential to be calculated for each Δt for *each synapse*. For the present algorithm, at each time step Δt, many fewer exponentials are calculated compared to the number of synapses.

Note that this algorithm can also be formulated for the case of multiple synapses with different conductances by introducing a multiplicative factor to each r_i in Eq. 35 according to its conductance value (see details in Lytton, 1996).

D Tutorials for implementing network simulations

We have developed tutorial simulations to illustrate the use of kinetic models for building network simulations. These tutorials can be obtained from the Internet at

http://www.cnl.salk.edu/~alain/

and are running on the publicly available NEURON simulator (Hines, 1993; see also Chapter 3, this volume).

Tutorial files are available for all models of synaptic currents described in this Chapter, including the presynaptic release model, as well as detailed and simplified kinetic models for AMPA, NMDA, $GABA_A$ and $GABA_B$ receptors. Other tutorials illustrate how to implement these models to simulate network of neurons. The simulations provided reproduce some of the figures of published papers (Destexhe et al, 1994a, 1996), in which a description of the biological background and the details of the ionic currents is given. A copy of these papers is also available on the Internet at the above address.

Acknowledgments

This research was supported by MRC (Medical Research Council of Canada), FRSQ (Fonds de la Recherche en Santé du Québec), HHMI (Howard Hughes Medical Institute), ONR (Office of Naval Research) and NIMH (National Institutes of Mental Health). We thank Drs. T. Brown, Y. De Koninck, N.A. Hessler, R. Malinow, I. Mody, T. Otis, and Z. Xiang for providing whole-cell recordings.

References

[1] Augustine, G.J. and Charlton, M.P. (1986) Calcium dependence of presynaptic calcium current and post-synaptic response at the squid giant synapse. *J. Physiol. (London)* **381**:619-640.

[2] Bal, T., von Krosigk, M. and McCormick, D.A. (1995a) Synaptic and membrane mechanisms underlying synchronized oscillations in the ferret lateral geniculate nucleus *in vitro*. *J. Physiol.* **483**: 641-663.

[3] Bal, T., von Krosigk, M. and McCormick, D.A. (1995b) Role of the ferret perigeniculate nucleus in the generation of synchronized oscillations *in vitro*. *J. Physiol.* **483**: 665-685.

[4] Bartol, T.M., Land, B.R., Salpeter, E.E. and Salpeter, M.M. (1991) Monte Carlo simulation of miniature endplate current generation in the vertebrate neuromuscular junction. *Biophys. J.* **59**: 1290-1307.

[5] Bartol T.M. and Sejnowski, T.J. (1993) Model of the quantal activation of NMDA receptors at a hippocampal synaptic spine. *Soc. Neurosci. Abstracts* **19**: 1515.

[6] Bartol, T.M., Stiles, J.R., Salpeter, M.M., Salpeter, E.E., and Sejnowski, T.J. (1996) MCELL: Generalized Monte Carlo computer simulation of synaptic transmission and chemical signaling. *Soc. Neurosci. Abstracts* **22**: 1742.

[7] Bliss, T.V. and Collingridge, G.L. (1993) A synaptic model of memory: long-term potentiation in the hippocampus. *Nature* **361**: 31-39.

[8] Brown. D.A. (1990) G-proteins and potassium currents in neurons. *Ann. Rev. Physiol.* **52**: 215-242.

[9] Brown, A.M. and Birnbaumer, L. (1990) Ionic channels and their regulation by G protein subunits. *Ann. Rev. Physiol.* **52**: 197-213.

[10] Burgard, E.C. and Hablitz, J.J. (1993) NMDA receptor-mediated components of miniature excitatory synaptic currents in developing rat neocortex. *J. Neurophysiol.* **70**: 1841-1852.

[11] Busch, C., Sakmann, B. (1990) Synaptic transmission in hippocampal neurons: numerical reconstruction of quantal IPSCs. *Cold Spring Harbor Symp. Quant. Biol.* **55**: 69-80.

[12] Celentano, J.J. and Wong, R.K. (1994) Multiphasic desensitization of the $GABA_A$ receptor in outside-out patches. *Biophys. J.* **66**: 1039-1050.

[13] Clements, J.D. (1996) Transmitter time course in the synaptic cleft: its role into central synaptic function. *Trends Neurosci.* **19**: 163-171.

[14] Clements, J.D., Lester, R.A.J., Tong, G., Jahr, C.E., and Westbrook, G.L. (1992) The time course of glutamate in the synaptic cleft. *Science* **258**: 1498-1501.

[15] Clements, J.D., Westbrook, G.L. (1991) Activation kinetics reveal the number of glutamate and glycine binding sites on the N-methyl-D-aspartate receptor. *Neuron* **258**: 605-613.

[16] Colquhoun, D., Jonas, P., and Sakmann, B. (1992) Action of brief pulses of glutamate on AMPA/Kainate receptors in patches from different neurons of rat hippocampal slices. *J. Physiol.* **458**, 261-287.

[17] Constantine-Paton, M., Cline, H.T. and Debski, E. (1990) Patterned activity, synaptic convergence, and the NMDA receptor in developing visual pathways. *Ann. Rev. Neurosci.* **13**: 129-154.

[18] Davies C.H., Davies, S.N. and Collingridge, G.L. (1990) Paired-pulse depression of monosynaptic GABA-mediated inhibitory postsynaptic responses in rat hippocampus. *J. Physiol.* **424**: 513-531.

[19] De Koninck, Y. and Mody, I. (1994) Noise analysis of miniature IPSCs in adult rat brain slices: properties and modulation of synaptic $GABA_A$ receptor channels. *J. Neurophysiol.* **71**: 1318-1335.

[20] Destexhe, A. (1997) Conductance-based integrate and fire models. *Neural Computation* **9**: 503-514.

[21] Destexhe, A., Bal, T., McCormick, D.A. and Sejnowski, T.J. (1996) Ionic mechanisms underlying synchronized oscillations and propagating waves in a model of ferret thalamic slices. *J. Neurophysiol.* **76**: 2049-2070.

[22] Destexhe, A., Contreras, D., Sejnowski, T.J. and Steriade, M. (1994a) A model of spindle rhythmicity in the isolated thalamic reticular nucleus. *J. Neurophysiol.* **72**: 803-818.

[23] Destexhe, A., Mainen, Z. and Sejnowski, T.J. (1994b) An Efficient Method for Computing Synaptic Conductances Based on a Kinetic Model of Receptor Binding. *Neural Computation* **6**: 14-18.

[24] Destexhe, A., Mainen, Z. and Sejnowski, T.J. (1994c) Synthesis of models for excitable membranes, synaptic transmission and neuromodulation using a common kinetic formalism. *J. Computational Neurosci.* **1**: 195-230.

[25] Destexhe, A. and Sejnowski, T.J. (1995) G-protein activation kinetics and spill-over of GABA may account for differences between inhibitory responses in the hippocampus and thalamus. *Proc. Natl. Acad. Sci. USA* **92**: 9515-9519.

[26] Dutar, P. and Nicoll, R.A. (1988) A physiological role for $GABA_B$ receptors in the central nervous system. *Nature* **332**: 156-158.

[27] Edmonds, B. and Colquhoun, D. (1993) Rapid decay of averaged single-channel NMDA receptor activations recorded at low agonist concentration. *Proc. Roy. Soc. Lond. Ser. B* **250**: 279-286.

[28] Franke, C., Hatt, H., and Dudel, J. (1987) Liquid filament switch for ultrafast exchanges of solutions at excised patches of synaptic membrane of crayfish muscle. *Neurosci. Lett.* **77**: 199-204.

[29] Geiger, J.R., Melcher, T., Koh, D.S., Sakmann, B., Seeburg, P.H., Jonas, P. and Monyer, H. (1995) Relative abundance of subunit mRNAs determines gating and Ca2+ permeability of AMPA receptors in principal neurons and interneurons in rat CNS. *Neuron* **15**: 193-204.

[30] Hessler, N.A., Shirke, A.M. and Malinow, R. (1993) The probability of transmitter release at a mammalian central synapse. *Nature* **366**: 569-572.

[31] Hestrin, S. (1992) Activation and desensitization of glutamate-activated channels mediating fast excitatory synaptic currents in the visual cortex. *Neuron* **9**: 991-999.

[32] Hestrin, S. (1993) Different glutamate receptor channels mediate fast excitatory synaptic currents in inhibitory and excitatory cortical neurons. *Neuron* **11**: 1083-1091.

[33] Hestrin, S. and Sah, P. and Nicoll, R. A. (1990) Mechanisms generating the time course of dual component excitatory synaptic currents recorded in hippocampal slices. *Neuron* **5**: 247-253.

[34] Hines, M. (1993) NEURON — A program for simulation of nerve equations. In: *Neural Systems: Analysis and Modeling.* F. Eeckman, editor. Kluwer Academic Publishers, Norwell, MA, pp 127-136.

[35] Hodgkin, A.L. and Huxley, A.F. (1952) A quantitative description of membrane current and its application to conduction and excitation in nerve. *J. Physiol.* **117**: 500-544.

[36] Huguenard, J.R. and Prince, D.A. (1994) Clonazepam suppresses $GABA_B$ -mediated inhibition in thalamic relay neurons through effects in nucleus reticularis. *J. Neurophysiol.* **71**: 2576-2581.

[37] Huntley, G.W., Vickers, J.C. and Morrison, J.H. (1994) Cellular and synaptic localization of NMDA and non-NMDA receptor subunits in neocortex: organizational features related to cortical circuitry, function and disease. *Trends Neurosci.* **17**: 536-543.

[38] Isaacson, J.S., Solis, J.M. and Nicoll, R.A. (1993) Local and diffuse synaptic actions of GABA in the hippocampus. *Neuron* **10**: 165-175.

[39] Jahr, C. E. (1992) High probability of opening of NMDA receptor channels by L-glutamate. *Science* **255**: 470-472.

[40] Jahr, C.E. and Stevens, C.F. (1990a) A quantitative description of NMDA receptor-channel kinetic behavior. *J. Neurosci.* **10**: 1830-1837.

[41] Jahr, C.E. and Stevens, C.F. (1990b) Voltage dependence of NMDA-activated macroscopic conductances predicted by single-channel kinetics. *J. Neurosci.* **10**: 3178-3182.

[42] Jonas, P., Major, G. and Sakmann, B. (1993) Quantal components of unitary EPSCs at the mossy fibre synapse on CA3 pyramidal cells of rat hippocampus. *J. Physiol.* **472**: 615-663.

[43] Jonas, P., Racca, C., Sakmann, B., Seeburg, P.H. and Monyer, H. (1994) Differences in Ca2+ permeability of AMPA-type glutamate receptor channels in neocortical neurons caused by differential GluR-B subunit expression. *Neuron* **12**: 1281-1289.

[44] Koh, D.S., Geiger, J.R., Jonas, P. and Sakmann, B. (1995) Ca(2+)-permeable AMPA and NMDA receptor channels in basket cells of rat hippocampal dentate gyrus. *J. Physiol.* **485**: 383-402.

[45] Lester, R. A. J., Clements, J. D., Westbrook, G. L. and Jahr, C. E. (1990) Channel kinetics determine the time course of NMDA receptor-mediated synaptic currents. *Nature* **346**: 565-567.

[46] Lester, R. A. J. and Jahr, C. E. (1992) NMDA channel behavior depends on agonist affinity. *J. Neurosci* bf 12: 635-643.

[47] Lytton, W.W. (1996) Optimizing synaptic conductance calculation for network simulations. *Neural Computation* **8**: 501-509.

[48] Markram, H. and Tsodyks, M. (1996) Redistribution of synaptic efficacy between neocortical pyramidal neurons. *Nature* **382**: 807-810.

[49] McBain, C. and Dingledine, R. (1992) Dual-component miniature excitatory synaptic currents in rat hippocampal CA3 pyramidal neurons. *J. Neurophysiol.* **68**: 16-27.

[50] McCormick, D.A. (1992) Neurotransmitter actions in the thalamus and cerebral cortex and their role in neuromodulation of thalamocortical activity. *Progress Neurobiol.* **39**: 337-388.

[51] McKernan, R.M. and Whiting, P.J. Which $GABA_A$-receptor subtypes really occur in the brain? *Trends Neurosci.* **19**: 139-143.

[52] Mody, I., De Koninck, Y., Otis, T.S. and Soltesz, I. (1994) Bridging the cleft at GABA synapses in the brain. *Trends Neurosci.* **17**: 517-525.

[53] Molinoff, P.B., Williams, K., Pritchett, D.B. and Zhong, J. (1994) Molecular pharmacology of NMDA receptors: modulatory role of NR2 subunits. *Prog. Brain Res.* **100**: 39-45.

[54] Monyer, H., Burnashev, N., Laurie, D.J., Sakmann, B. and Seeburg, P.H. (1994) Developmental and regional expression in the rat brain and functional properties of four NMDA receptors. *Neuron* **12**: 529-540.

[55] Mosbacher, J., Schoepfer, R., Monyer, H., Burnashev, N., Seeburg, P.H. and Ruppersberg, J.P. (1994) A molecular determinant for submillisecond desensitization in glutamate receptors. *Science* **266**: 1059-1062.

[56] Nowak, L., Bregestovski, P., Ascher, P., Herbet, A. and Prochiantz, A. (1984) Magnesium gates glutamate-activated channels in mouse central neurones. *Nature* **307**: 462-465.

[57] Otis, T.S., De Koninck, Y. and Mody, I. Whole-cell recordings of evoked and spontaneous $GABA_B$ responses in hippocampal slices. *Pharmacol. Commun.* **2**: 75-83, 1992.

[58] Otis, T.S., De Koninck, Y. and Mody, I. (1993) Characterization of synaptically elicited $GABA_B$ responses using patch-clamp recordings in rat hippocampal slices. *J. Physiol.* **463**: 391-407.

[59] Otis, T.S. and Mody, I. (1992) Modulation of decay kinetics and frequency of $GABA_A$ receptor-mediated spontaneous inhibitory postsynaptic currents in hippocampal neurons. *Neuroscience* **49**: 13-32.

[60] Patneau, D.K. and Mayer, M.L. (1991) Kinetic analysis of interactions between kainate and AMPA: evidence for activation of a single receptor in mouse hippocampal neurons. *Neuron* **6**: 785-798.

[61] Press, W.H., Flannery, B.P., Teukolsky, S.A. and Vetterling, W.T. (1986) *Numerical Recipes. The Art of Scientific Computing.* Cambridge University Press, Cambridge, MA.

[62] Rall, W. (1967) Distinguishing theoretical synaptic potentials computed for different soma-dendritic distributions of synaptic inputs. *J. Neurophysiol.* **30**, 1138–1168.

[63] Raman, I.M. and Trussell, L.O. (1992) The kinetics of the response to glutamate and kainate in neurons of the avian cochlear nucleus. *Neuron* **9**:173-186.

[64] Raman, I.M., Zhang, S. and Trussell, L.O. (1994) Pathway-specific variants of AMPA receptors and their contribution to neuronal signaling. *J. Neurosci.* **14**: 4998-5010.

[65] Ropert, N., Miles, R. and Korn, H. (1990) Characteristics of miniature inhibitory postsynaptic currents in CA1 pyramidal neurones of rat hippocampus. *J. Physiol.* **428**: 707-722.

[66] Sakmann, B. and Neher, E. (Editors) (1995) *Single-Channel Recording* (2nd edition). Plenum Press, New York, NY.

[67] Schoepfer, R., Monyer, H., Sommer, B., Wisden, W., Sprengel, R., Kuner, T., Lomeli, H., Herb, A., Kohler, M., Burnashev, N. et al. Molecular biology of glutamate receptors. *Progress Neurobiol.* **42**: 353-357.

[68] Schweizer, F.E., Betz, H. and Augustine, G.J. (1995) From vesicle docking to endocytosis: intermediate reactions of exocytosis. *Neuron* **14**: 689-696.

[69] Spruston, N., Jonas, P. and Sakmann, B. (1994) Dendritic glutamate receptor channels in rat hippocampal CA3 and CA1 pyramidal neurons. *J. Physiol.* **482**: 325-352.

[70] Stiles, J.R., Van Helden, D., Bartol, T.M., Salpeter, E.E. and Salpeter, M.M. (1996) Miniature endplate current rise times less than 100 microseconds from improved dual recordings can be modeled with passive acetylcholine diffusion from a synaptic vesicle. *Proc. Natl. Acad. Sci. USA* **93**: 5747-5752.

[71] Srinivasan, R., and Chiel, H.J. (1993) Fast calculation of synaptic conductances. *Neural Computation* **5**, 200-204.

[72] Standley, C., Ramsey, R.L. and Usherwood, P.N.R. (1993) Gating kinetics of the quisqualate-sensitive glutamate receptor of locust muscle studied using agonist concentration jumps and computer simulations. *Biophys. J.* **65**: 1379-1386.

[73] Steriade, M., McCormick, D.A. and Sejnowski., T.J. (1993) Thalamocortical oscillations in the sleeping and aroused brain. *Science* **262**: 679-685.

[74] Stevens, C.F. (1978) Interactions between intrinsic membrane protein and electric field. *Biophys. J.* **22**: 295-306.

[75] Stevens, C.F. and Wang, Y. (1995) Facilitation and depression at single central synapses. *Neuron* **14**: 795-802.

[76] Stricker, C., Field, A.C. and Redman, S.J. (1996) Statistical analysis of amplitude fluctuations in EPSCs evoked in rat CA1 pyramidal neurones in vitro. *J. Physiol.* **490**: 419-441.

[77] Thompson, S.M. (1994) Modulation of inhibitory synaptic transmission in the hippocampus. *Progress Neurobiol.* **42**: 575-609.

[78] Thompson, S.M. and Gähwiler, B.H. (1992) Effects of the GABA uptake inhibitor tiagabine on inhibitory synaptic potentials in rat hippocampal slice cultures. *J. Neurophysiol.* **67**: 1698-1701.

[79] Thomson, A.M. and Deuchars, J. (1994) Temporal and spatial properties of local circuits in neocortex. *Trends Neurosci.* **17**:119-126.

[80] Wang, X.J. and Rinzel, J. Alternating and synchronous rhythms in reciprocally inhibitory model neurons. *Neural Computation* **4**: 84-97, 1992.

[81] Xiang, Z., Greenwood, A.C. and Brown, T. (1992) Measurement and analysis of hippocampal mossy-fiber synapses (abstract). *Soc. Neurosci. Abstracts* **18**: 1350.

[82] Yamada, W.M. and Zucker, R.S. (1992) Time course of transmitter release calculated from simulations of a calcium diffusion model. *Biophys. J.* **61**: 671-682.

[83] Zhang, S. and Trussell, L.O. (1994) Voltage clamp analysis of excitatory synaptic transmission in the avian nucleus magnocellularis. *J. Physiol.* **480**: 123-136.

[84] Zukin, R.S. and Bennett, M.V. (1995) Alternatively spliced isoforms of the NMDARI receptor subunit. *Trends Neurosci.* **18**: 306-313.